AIAA Meeting Papers on Disc, May 1996
A9630781, NAG1-1367, AIAA Paper 96-1663

A time-domain implementation of surface acoustic impedance condition with and without flow

Yusuf Ozyoruk
Pennsylvania State Univ. University Park

Lyle N. Long
Pennsylvania State Univ. University Park

AIAA and CEAS, Aeroacoustics Conference, 2nd, State College, PA, May 6-8, 1996

The impedance condition in computational aeroacoustic applications is required in order to model acoustically treated walls. The application of this condition in time-domain methods, however, is extremely difficult because of the convolutions involved. In this paper, a time-domain method is developed which overcomes the computational difficulties associated with these convolutions. This method builds on the z-transform from control and signal processing theory and the z-domain model of the impedance. The idea of using the z-domain operations originates from the computational electromagnetics community. When the impedance is expressed in the z-domain with a rational function, the inverse z-transform of the impedance condition results in only infinite impulse response type, digital, recursive filter operations. These operations, unlike convolutions, require only limited past-time knowledge of the acoustic pressures and velocities on the surface. One- and two-dimensional example problems with and without flow indicate that the method promises success for aeroacoustic applications. (Author)

96-1663
A96-30781

A Time-Domain Implementation of Surface Acoustic Impedance Condition with and without Flow

Yusuf Özyörük* and Lyle N. Long†
Department of Aerospace Engineering
The Pennsylvania State University, University Park, PA 16802

Abstract

The impedance condition in computational aeroacoustic applications is required in order to model acoustically treated walls. The application of this condition in time-domain methods, however, is extremely difficult because of the convolutions involved. In this paper, a time-domain method is developed which overcomes the computational difficulties associated with these convolutions. This method builds on the z-transform from control and signal processing theory and the z-domain model of the impedance. The idea of using the z-domain operations originates from the computational electromagnetics community. When the impedance is expressed in the z-domain with a rational function, the inverse z-transform of the impedance condition results in only infinite impulse response type, digital, recursive filter operations. These operations, unlike convolutions, require only limited past-time knowledge of the acoustic pressures and velocities on the surface. One- and two-dimensional example problems with and without flow indicate that the method promises success for aeroacoustic applications.

1 Introduction

The surface impedance condition in computational aeroacoustic (CAA) applications, such as the calculation of sound propagation through an engine inlet duct,[1–4] is extremely important. Relatively quiet modern turbofan engines rely heavily on acoustic treatment (liners) on the inlet wall.[5] Sound waves are absorbed by the liner material to a degree depending upon the frequency content of the waves. Thus part of the inlet noise is suppressed.

In order to calculate sound propagation over acoustically treated surfaces in the time domain, the impedance condition has to be properly formulated. To the authors' knowledge, no time-domain implementations of the acoustic impedance condition on surfaces with or without flow have been reported to date. This is due to the fact that impedance conditions are best dealt with in the frequency domain because the acoustic response on a surface is a function of the wave frequency.[5] However, the frequency-domain methods,[6] unlike the time-domain methods, can only solve single frequency problems one at a time. Expensive convolutions are required in time-domain applications, however, due to the frequency-dependent characteristics of the lining materials.

This paper addresses the time-domain impedance conditions exploiting the ideas of digital filter applications of signal processing theory[7] for efficient implementations in CAA applications. The z-transform is used to formulate the impedance condition in the z-domain, and the impedance is modeled by a rational function in z. Then an inverse z-transform to the time domain provides the time-discretized impedance condition. This approach was used successfully by the computational electromagnetics (CEM) community[8,9] to establish a simple yet efficient tool for including the impedance condition as only infinite impulse response (IIR) type, digital filter operations[7] between the magnetic and electric fields (input/output). However, there are complications in CAA because of the convective flow effects. This is particularly true when the impedance is allowed to vary on the wall. The complication in the z-transform application is associated with the gradient of the rational function representation of the impedance in the equations. Therefore, the impedance in this paper is assumed to be independent of the location on the surface.

The time-domain impedance condition is derived starting from the frequency-domain formulation of Myers.[10] This is discussed in the next section. Then the z-transform procedure is introduced, which is followed by the discussion of the numerical implementation in a time-integration scheme. Then one and two-dimensional test cases are discussed. The two dimensional case involves the reflection of a Gaussian pulse from a flat plate in uniform flow. The results indicate that the current method has promise for further developments and applications.

*Post-Doctoral Scholar, Member, AIAA
†Associate Professor, Senior Member, AIAA

2 Impedance Condition

Myers[10] derived a general acoustic impedance boundary condition assuming that a soft wall (acoustically treated surface) undergoes deformations in response to an incident acoustic field from the fluid. He assumed these deformations are small perturbations to a stationary mean surface, and the corresponding fluid velocity field is a small perturbation about a mean base flow $\mathbf{V}_m$. His linearized, frequency-domain impedance (with an $e^{i\omega t}$ time dependence) can be expressed as

$$\hat{\mathbf{V}}(\omega)\cdot\mathbf{n} = -\hat{p}(\omega)/Z(\omega) - (1/i\omega)\,\mathbf{V}_m\cdot\nabla[\hat{p}(\omega)/Z(\omega)] + \mathbf{n}\cdot(\mathbf{n}\cdot\nabla\mathbf{V}_m)\,[\hat{p}(\omega)/i\omega Z(\omega)] \qquad (1)$$

where $\hat{\mathbf{V}}$ is the complex amplitude of the velocity perturbation, ω is the circular frequency, $\mathbf{n}$ is the mean surface normal, $\hat{p}$ is the complex amplitude of the pressure perturbation, Z is the impedance, $i = \sqrt{-1}$, and $\mathbf{V}_m$ is the mean velocity about which the linearization is performed. The use of this condition is restricted to linear unsteady flow situations due to the assumptions made in its derivation. The impedance is usually given by

$$Z(\omega) = R(\omega) + i\,X(\omega) \qquad (2)$$

where $R(\omega)$ and $X(\omega)$ are the frequency-dependent resistance and reactance, respectively, of the lining material. The impedance surface is assumed locally reacting.[5,11] That is, the behavior of the lining material is independent of the detailed nature of the acoustic pressure in the surrounding.

It is clear from Eq. (1) that in the absence of flow, the impedance condition reduces to

$$\hat{\mathbf{V}}(\omega)\cdot\mathbf{n} = -\hat{p}(\omega)/Z(\omega), \quad \text{soft wall; no flow,} \qquad (3)$$
$$\hat{\mathbf{V}}(\omega)\cdot\mathbf{n} = 0 \quad \text{hard wall} \qquad (4)$$

These equations are rather easy to implement in a frequency-domain method. A time-domain implementation, however, requires the inverse Fourier transform of the impedance condition, which results in a convolution equation. For example, transforming the impedance condition given for the no-flow case we arrive at the equation

$$p'(t) = -\int_0^t Z(t-\tau)\;\mathbf{n}\cdot\mathbf{V}'(\tau)\,d\tau \qquad (5)$$

where now the impedance must be expressed in the time domain and the past time history of the normal velocity perturbation $\mathbf{n}\cdot\mathbf{V}' = v_n'$ at the wall must be provided in order to evaluate the integral.

The time-domain impedance condition in the presence of flow becomes more difficult to deal with. Assuming the impedance is independent of the surface location and multiplying through Eq. (1) by $i\omega Z(\omega)$, we can write

$$i\omega\hat{p}(\omega) + \mathbf{V}_m\cdot\nabla\hat{p}(\omega) - \mathbf{n}\cdot(\mathbf{n}\cdot\nabla\mathbf{V}_m)\,\hat{p}(\omega) = -[i\omega Z(\omega)]\,[\hat{v}_n(\omega)] \qquad (6)$$

After the inverse Fourier transform, we obtain

$$\frac{\partial}{\partial t}p'(t) + \mathbf{V}_m\cdot\nabla p'(t) - \mathbf{n}\cdot(\mathbf{n}\cdot\nabla\mathbf{V}_m)\,p'(t) = -\int_0^t v_n'(\tau)\,[\frac{\partial}{\partial\tau}Z(\tau)]|_{t-\tau}\,d\tau \qquad (7)$$

A convolution integral is usually evaluated numerically with a simple summation formula over the discrete time range $0,...,n\Delta t$, where Δt is the time increment. For example, the right-hand side of Eq. (7) can be computed using

$$\int_0^t v_n'(\tau)\frac{\partial Z(\tau)}{\partial\tau}|_{t-\tau}\,d\tau \cong \Delta t\sum_{m=0}^{n} v_n'[m\Delta t]\dot{Z}[(n-m)\Delta t] \qquad (8)$$

This equation evidently indicates a need for significant computational resources for problems over long time periods, typical to CAA. If the calculations are being carried out for 10,000 time steps, for example, on a 128×128 surface mesh, Eq. (8) requires an array of size (10000,200,200) for the acoustic velocity v_n'. Hence the evaluation of the above convolution integral is computationally expensive and consequently impractical for multi-dimensional CAA problems. Moreover, the time accuracy of Eq. (8) is usually hindered by the above simple summation approach. This fact will be demonstrated by an example later.

3 The z-Transform

The z-transform procedure is used in the CEM community[8,9] to overcome the difficulties associated with the convolution integrals of the impedance condition. One can consider the impedance term that appears in the convolution integral of Eq. (5) or Eq. (7) as the acoustic system's response to the acoustic normal velocity input, and the integrals as the output. The idea here is then to represent the discrete form of the output (e.g. the summation in Eq. (8)) as a linear combination of the previous inputs and outputs. By this approach one can find an equivalent finite series to a convolution summation. The z-transform is a useful tool to accomplish this task. If the impedance Z can be expressed as a fraction of two finite polynomials in the complex variable z, this goal is achieved easily. This procedure is described with an example below. First we give the definition of the z-transform.

If $q(t)$ is a time-continuous variable, its discrete form is given by

$$q[n] = q(t)\,\delta(t - n\Delta t), \quad -\infty \leq n \leq +\infty \tag{9}$$

where $\delta()$ is the Dirac delta function. Then the definition of the z-transform is[8]

$$\mathcal{Z}\{q[n]\} = Q(z) = \Delta t \sum_{n=-\infty}^{\infty} q[n]\, z^{-n} \tag{10}$$

where $Q(z)$ is the z-transform of the sequence $q[n]$. Similar definitions are also possible.[7] Thus, if $h(t)$ is time-continuous data given, for example, by

$$h(t) = \frac{1}{t_0} e^{-t/t_0}, \quad t \geq 0, \tag{11}$$

the z-transform of its discrete form is

$$\begin{aligned}\mathcal{Z}\{h[n]\} = H(z) &= \frac{\Delta t}{t_0} \sum_{n=0}^{\infty} \left[e^{-\Delta t/t_0} z^{-1} \right]^n \\ &= \frac{\Delta t / t_0}{1 - e^{-\Delta t/t_0}\, z^{-1}}\end{aligned} \tag{12}$$

The z-transforms have common properties with the Fourier transforms, such as convolution, shifting, etc. Thus

$$\mathcal{Z}\{q[(n-1)\Delta t]\} = z^{-1} Q(z) \tag{13}$$

is the shifting property that will be used below.

A time derivative can be approximated by a first-order backward difference as

$$\frac{d}{dt} q(t) = \frac{q[n\Delta t] - q[(n-1)\Delta t]}{\Delta t} \tag{14}$$

The z-transform of this is then given by

$$\mathcal{Z}\{\frac{d}{dt} q(t)\} = \frac{1 - z^{-1}}{\Delta t} Q(z) \tag{15}$$

Now since $e^{i\omega} \longleftrightarrow z$, the no-flow impedance condition, for example, given by Eq. (3) can be written in the z-domain simply as

$$P(z) = -Z(z)\, V_n(z) \tag{16}$$

where $P(z)$ is the z-transform of the acoustic pressure, $Z(z)$ is the z-transform of the impedance, and $V_n(z)$ is the z-transform of the acoustic normal velocity at the wall.

Hence, if we knew the z-transform of the impedance in terms of the ratio of two finite polynomials in z, like the one given by Eq. (12), using the shifting property of the z-transform (Eq. (13)), we could obtain a simple relation between the acoustic velocity and pressure. For example, let $Z(z)$ be given by

$$Z(z) = \frac{a_0 + a_1 z^{-1}}{1 - b_1 z^{-1} - b_2 z^{-2}} \tag{17}$$

where a's and b's are some constants. Then, the substitution of Eq. (17) into Eq. (16) yields

$$(1 - b_1 z^{-1} - b_2 z^{-2}) P(z) = -(a_0 + a_1 z^{-1}) V_n(z) \tag{18}$$

Then after the inverse z-transform using the shifting property (Eq. (13)), we obtain

$$p^n = b_1 p^{n-1} + b_2 p^{n-2} - (a_0 v_n^n + a_1 v_n^{n-1}) \tag{19}$$

where now the superscript n indicates the time level, a common notation used in CFD and CAA. The left-hand side of the above equation is, therefore, nothing but the current time output of the acoustic system as a function of the previous outputs and inputs as well as the current acoustic velocity input. Thus the right-hand side is analogous to a digital filter, specifically to a recursive, IIR filter.[7] Thus a very simple connection is established between the discrete acoustic pressure and the normal velocity on the surface.

4 Impedance Condition in the z-Domain

In order for the more general frequency-domain impedance condition given by Eq. (6) to be formulated in the z-domain, we simply use the following derivative operator relations:

$$\frac{\partial}{\partial t} \stackrel{\mathcal{F}}{=} i\omega \stackrel{\mathcal{Z}}{=} \frac{1 - z^{-1}}{\Delta t} \tag{20}$$

where $\mathcal{F}$ is the Fourier transform operator. A bilinear approximation can also be used:

$$i\omega \stackrel{\mathcal{Z}}{=} \frac{2}{\Delta t} \frac{1 - z^{-1}}{1 + z^{-1}} \tag{21}$$

However, the following discussion and derivations will use the backward difference approach (Eq. (20)). Then by the substitution of Eq. (20), the impedance condition (Eq. (6)) can be expressed in the z-domain as

$$\begin{aligned}\frac{1 - z^{-1}}{\Delta t} P(z) + \mathbf{V}_m \cdot \nabla P(z) - \mathbf{n} \cdot (\mathbf{n} \cdot \nabla \mathbf{V}_m)\, P(z) \\ = -\frac{1 - z^{-1}}{\Delta t} Z(z)\, V_n(z)\end{aligned} \tag{22}$$

Now let the z-transform of the impedance be modeled in general by

$$Z(z) = \frac{a_0 + \sum_{\ell=1}^{M_N} a_\ell z^{-\ell}}{1 - \sum_{k=1}^{M_D} b_k z^{-k}} \tag{23}$$

where a's and b's are the constants that give the best approximation to the impedance. For stability, the poles of $Z(z)$ must be in the upper half of the complex plane.[7] After the substitution of this $Z(z)$ into Eq. (22) and some algebra and manipulation, we obtain

$$\frac{1-z^{-1}}{\Delta t}P(z) + \mathbf{V}_m \cdot \nabla P(z) - \mathbf{n}\cdot(\mathbf{n}\cdot\nabla\mathbf{V}_m)P(z) = -a_0\frac{1-z^{-1}}{\Delta t}V_n(z) + \bar{R} \tag{24}$$

where

$$\begin{aligned}\bar{R} &= -\frac{1}{\Delta t}\sum_{\ell=1}^{M_N} a_\ell(z^{-\ell} - z^{-\ell-1})V_n(z) \\ &+ \frac{1}{\Delta t}\sum_{k=1}^{M_D} b_k(z^{-k} - z^{-k-1})P(z) \\ &+ \mathbf{V}_m \cdot \nabla \sum_{k=1}^{M_D} b_k z^{-k}P(z) \\ &- \mathbf{n}\cdot(\mathbf{n}\cdot\nabla\mathbf{V}_m)\sum_{k=1}^{M_D} b_k z^{-k}P(z)\end{aligned} \tag{25}$$

Then the multiplication of Eq. (24) by z and a consequent inverse z-transform of it result in the following time-discretized impedance condition

$$\frac{p^{n+1}-p^n}{\Delta t} + \mathbf{V}_m \cdot \nabla p^{n+1} - \mathbf{n}\cdot(\mathbf{n}\cdot\nabla\mathbf{V}_m)p^{n+1} = -a_0\frac{v_n^{n+1}-v_n^n}{\Delta t} + R^{n,n-1,\ldots} \tag{26}$$

where

$$\begin{aligned}R^{n,n-1,\ldots} &= -\frac{1}{\Delta t}\sum_{\ell=1}^{M_N} a_\ell(v_n^{n+1-\ell} - v_n^{n-\ell}) \\ &+ \frac{1}{\Delta t}\sum_{k=1}^{M_D} b_k(p^{n+1-k} - p^{n-k}) \\ &+ \mathbf{V}_m \cdot \nabla \sum_{k=1}^{M_D} b_k p^{n+1-k} \\ &- \mathbf{n}\cdot(\mathbf{n}\cdot\nabla\mathbf{V}_m)\sum_{k=1}^{M_D} b_k p^{n+1-k}\end{aligned} \tag{27}$$

where p and v_n are the acoustic pressure and normal velocity on the wall, respectively. This equation requires the mean flow information. Note that on the surface the mean flow satisfies

$$\mathbf{n}\cdot\mathbf{V}_m = 0 \tag{28}$$

Therefore, if the impedance condition is formulated on a body-fitted orthogonal coordinate system (ξ,η,ζ) with η emanating from the surface, the $\mathbf{V}_m\cdot\nabla p$ term becomes

$$\mathbf{V}_m \cdot \nabla p = \bar{U}_m\frac{\partial p}{\partial \xi} + \bar{W}_m\frac{\partial p}{\partial \zeta} \tag{29}$$

where $\bar{U}_m$ and $\bar{W}_m$ are the contravariant mean velocities in the ξ and ζ directions, respectively. If the ζ curves are the azimuthal grid lines of a mesh around an engine inlet, for example, the mean velocity $\bar{W}_m$ is usually small compared to $\bar{U}_m$, except around the stagnation points, and identically zero for axisymmetric mean flows. Therefore, the product $\bar{W}_m\partial p/\partial\zeta$ could be negligible on most of the acoustically treated regions of the engine inlet wall. Also, the $\mathbf{n}\cdot(\mathbf{n}\cdot\nabla\mathbf{V}_m)$ is usually small where the curvature of the wall does not change significantly. Thus, the above impedance condition can be simplified significantly. The negligence of $\bar{W}_m\partial p/\partial\zeta$ is far more important because the spatial discretization of Eq. (26) yields a linear system of equations on the surface, as will be seen later.

In general, the solution of Eq. (26) for the current time step acoustic pressure, p^{n+1}, requires the current time step acoustic velocity, v_n^{n+1}, and the acoustic pressure and velocity histories of lengths M_D and M_N, respectively, where M_D is the number of the constant b's, and M_N is the number of a's in the z-domain impedance model. The modeling of the z-domain impedance and the incorporation of the impedance condition in a time-accurate aeroacoustic method are discussed in the following sections.

5 Numerical Implementation

5.1 Modeling of Impedance

The impedance has to be modeled first in the z-domain in order to apply the above boundary condition in a numerical algorithm. The frequency-dependent behavior of the resistance and reactance must be provided accurately in the frequency range of interest. Substituting z^{-1} from the backward difference relation given by Eq. (20), we can show that the resistance and reactance of the impedance must satisfy two equations of the form, respectively,

$$\frac{R(\omega)}{\rho c} = \frac{\tilde{a}_0 + \tilde{a}_1\omega^2 + \tilde{a}_2\omega^4 + \ldots}{\tilde{b}_0 + \tilde{b}_1\omega^2 + \tilde{b}_2\omega^4 + \ldots} \tag{30}$$

$$\frac{X(\omega)}{\rho c} = \frac{\tilde{c}_1\omega + \tilde{c}_2\omega^3 + \tilde{c}_3\omega^5 + \ldots}{\tilde{d}_0 + \tilde{d}_1\omega^2 + \tilde{d}_2\omega^4 + \ldots} \tag{31}$$

where $\tilde{a}, \tilde{b}, \tilde{c}$ and $\tilde{d}$ are constants that give the best resistance and reactance. Notice that the resistance is an even function and the reactance is an odd function of the circular frequency ω. The reason for this is that when $\omega = i\,(z^{-1}-1)/\Delta t$ is substituted into the above models, we remove the i dependence from the z-domain impedance so that it becomes

$$Z(z) = R(z) + X(z) \tag{32}$$

Hence the corresponding a's and b's of Eq. (23) are easily identified. Figure 1 shows the frequency-dependent behavior of a typical lining material. The symbols represent the experimental data of Motsinger and Kraft[5] and the curves are the results of a nonlinear least square fit[12] of the above two rational functions representing the resistance and reactance.

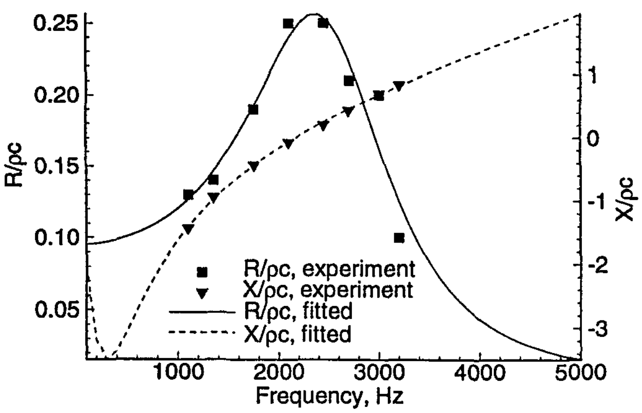

Figure 1: Resistance and reactance of a 6.7% perforate plate (at $M = 0$ and 126 dB incident sound). Experimental data is from Motsinger and Kraft.[5]

5.2 Time Integration

CAA problems are usually solved using high-order accurate, explicit, finite-difference, time-marching techniques. The hybrid ducted fan noise method of Özyörük and Long,[2,3] for example, uses a fourth-order accurate Runge-Kutta (R-K) time-integration scheme to integrate the three-dimensional, time-dependent Euler and nonreflecting boundary conditions equations. Since the time-discretized impedance condition (Eq. (26)) requires the full-time step solutions p^{n+1} and v^{n+1} on the acoustically treated wall, the application of the wall boundary conditions in an R-K scheme is of a special interest in this section. If the semi-discretized governing equations are given as

$$\frac{d\mathbf{Q}}{dt} = -[\mathcal{H}(\mathbf{Q}) - \mathcal{D}(\mathbf{Q})], \tag{33}$$

the R-K scheme (compact[13]) is then given by

$$\begin{aligned} \mathbf{Q}^{(1)} &= \mathbf{Q}^n, \\ \mathbf{Q}^{(s)} &= \mathbf{Q}^n - \alpha_s \Delta t\, [\mathcal{H}(\mathbf{Q}^{(s-1)}) - \mathcal{D}(\mathbf{Q}^{(1)})], \\ \mathbf{Q}^{n+1} &= \mathbf{Q}^{(4)} \end{aligned} \tag{34}$$

where $\mathbf{Q}$ is the vector of dependent solution variables, $\mathcal{H}(\mathbf{Q})$ is the collection of the spatial derivatives, $\mathcal{D}(\mathbf{Q})$ is artificial dissipation, and Δt is the time increment from one step to the next, and $\alpha_s = [1/4, 1/3, 1/2, 1]$.

First we discuss the hard-wall case ($Z(\omega) = \infty$). In this case, the wall boundary condition for the Euler calculations is that the normal velocity on the wall vanish. That is, $\mathbf{V} \cdot \mathbf{n} = 0$. Theoretically the other variables can be solved from the interior equations. However, within an R-K iteration the following solution procedure is usually applied for the entire computational domain.

Do s=1, RK_stages
-Update interior, $\mathbf{Q}^{(s)}$
-Update far field, $\mathbf{Q}'^{(s)}$
-Set $v_n^{(s)} = 0$ on wall
-Extrapolate $\rho^{(s)}, v_t^{(s)}$ from interior onto wall
-Solve normal momentum equation for $p_{wall}^{(s)}$
-Obtain $\rho e^{(s)}$ from equation of state on wall
End Do

where v_n and v_t are the normal and tangential components of the total velocity on the wall.

However, the impedance condition states that there is transpiration of mass into or out of the wall. That is, $\mathbf{V} \cdot \mathbf{n} \neq 0$ anymore. The amount of mass transpiration is fixed by the impedance of the wall. Therefore, instead of simple extrapolation of the density and the tangential velocities we simply use the interior equations to solve for these quantities. The normal velocity in this case can also be solved using the interior equations. However, since the impedance condition has resulted in an implicit relation between the acoustic pressure and normal velocity on the wall, either the acoustic pressure or normal velocity at the current time level $n+1$ (full time step) must be provided by the flow solver. The other is obtained from the impedance condition. Therefore, the application of the impedance condition in the R-K stages presents a difficulty as associated with the intermediate solutions being advanced by fractions of the time step size. We overcome this difficulty by assuming that the acoustic velocity $v_n^{(s)}$ is the available value of v_n^{n+1} and this is then substituted into the impedance condition for v_n^{n+1} to obtain $p^{(s)}$ as the available value of p^{n+1} on the wall. This then poses the question what Δt must be used in approximating $i\omega$ by $(1 - z^{-1})/\Delta t$ in the z-transform procedure. The answer to this is given in the results section by numerical experimentation.

It should be noted that the acoustic velocity $v_n^{(s)}$ (assumed to be the available value of v_n^{n+1}) required on the wall by the impedance condition can be obtained explicitly by solving the interior equations via the R-K scheme itself. However, as will be demonstrated later, in some cases this may result in a numerical instability at the wall. However, we leave this procedure as an option in our calculations. A superior treatment is the discretization of the normal momentum equation implicitly within the R-K stage and its simultaneous solution with the impedance condition equation.

Another significant issue is the solution of the impedance condition equation for the acoustic pressure in the presence of flow. When this equation is discretized in space, the result is a linear system of equations arising from the $\mathbf{V}_m \cdot \nabla p^{n+1}$ term, which is equivalent to the tangential gradient of the acoustic pressure since $\mathbf{n} \cdot \mathbf{V}_m = 0$ on the wall. This system of equations has to be inverted at every R-K stage.

Thus, in the case of acoustic treatment on the wall, an R-K iteration involves the following procedure in general:

Do s=1, RK_stages
- **-Update interior, $\mathbf{Q}^{(s)}$**
- **-Update far field, $\mathbf{Q}'^{(s)}$**
- **-Update $\rho^{(s)}$, $v_t^{(s)}$ at wall using interior eqs.**
- **-At wall, solve for $v_n^{(s)}$ using either**
  - **a) ONLY interior equations (explicit)**
  - **b) or interior equations PLUS the impedance condition (implicit)**
- **-Solve for $p_{wall}^{(s)}$ using the impedance cond.**
- **-Obtain $\rho e^{(s)}$ from equation of state at wall**

End Do

We consider only one and two-dimensional inviscid problems in this paper to address various numerical issues. These cases involve the reflection of broadband acoustic pulses from acoustically treated walls. Three-dimensional cases can be solved in a similar manner.

5.3 One-dimensional cases

The one dimensional cases involve acoustic pulse problems in a semi-infinite domain ($x > 0$) with an acoustic treatment at $x = 0$. Of course in this case there is no flow and any term involving $\mathbf{V}_m$ in the impedance expression given by Eq. (26) vanishes. The one-dimensional Euler equations are solved for the interior points, and one-dimensional nonreflecting boundary conditions are applied at $x = x_B$. The perturbation quantities in this case are ρ, u, p. Thus, the impedance condition (Eq. (26)) on the wall requires

$$p^{n+1} = -a_0(u^{n+1} - u^n) - \sum_{\ell=1}^{M_N} a_\ell(u^{n+1-\ell} - u^{n-\ell}) + p^n + \sum_{k=1}^{M_D} b_k(p^{n+1-k} - p^{n-k}) \quad (35)$$

Clearly the right-hand side of this equation is the approximation to the right-hand side (convolution) of Eq. (5) with $t = n\Delta t$. As indicated earlier, we consider $u^{(s)}$ as the available value of u^{n+1} in order to incorporate this equation in the R-K scheme, where the superscript (s) represents an R-K stage. Thus the acoustic velocity is obtained from the time-discretized linear momentum equation at the wall:

$$u^{(s)} - u^n = -\Delta t^* \frac{1}{\rho_\infty}\frac{\partial p^*}{\partial x} \quad (36)$$

where the superscript $*$ indicates that the evaluation stage is optional for the derivative term at this point and Δt^* will depend on this option. If the term $\partial p^*/\partial x$ is discretized at the R-K stage (s), Eq. (36) gives an implicit relation between acoustic pressure and velocity. In this case the time increment Δt^* can be taken as either Δt or $\alpha_s \Delta t$. The effects of these will be discussed in the results section. However, the evaluation of the above spatial derivative with values from the previous stage, i.e. $(s-1)$, results in an explicit solution of the acoustic velocity. In this case the R-K scheme is used, as is, to obtain the velocity. In both the explicit and implicit discretization cases $u^{(s)}$ is substituted into Eq. (35) for u^{n+1} to obtain the acoustic pressure p^{n+1} (equivalent to $p^{(s)}$).

5.4 Two-dimensional cases

The two-dimensional cases involve acoustic pulse problems in a semi-infinite plane ($-\infty < x < +\infty, y > 0$) with an acoustic treatment (soft wall) at $y = 0$. This domain is truncated to finite size using nonreflecting boundary conditions. In flow cases the mean flow is assumed to be uniform and in the direction of $+x$. That is, $\mathbf{Q}_m = [\rho_\infty, u_\infty, 0, (\rho e)_\infty]^T$. Thus, the impedance condition (Eq. (26)) at the wall requires

$$\frac{p^{(s)} - p^n}{\Delta t} + u_\infty \frac{\partial p^{(s)}}{\partial x} = -a_0 \frac{v^{(s)} - v^n}{\Delta t} + R^{n,n-1,\dots} \quad (37)$$

where

$$\begin{aligned} R^{n,n-1,\dots} &= -\frac{1}{\Delta t}\sum_{\ell=1}^{M_N} a_\ell(v^{n+1-\ell} - v^{n-\ell}) \\ &+ \frac{1}{\Delta t}\sum_{k=1}^{M_D} b_k(p^{n+1-k} - p^{n-k}) \\ &+ u_\infty \sum_{k=1}^{M_D} b_k \frac{\partial p^{n+1-k}}{\partial x} \end{aligned} \quad (38)$$

Now the right-hand side of Eq. (37) is an approximation to the right-hand side of Eq. (7). Similarly to the one-dimensional case, the acoustic velocity and the pressure at the time level $n+1$ are in an implicit relation. Therefore, the normal momentum equation is again used. In the case of small perturbations in the domain, the linearized y-momentum equation can be used. The discretized form of this equation is

$$\frac{v^{(s)} - v^n}{\Delta t^*} + u_\infty \frac{\partial v^*}{\partial x} + \frac{1}{\rho_\infty}\frac{\partial p^*}{\partial y} = 0 \quad (39)$$

This equation can be solved explicitly using the R-K scheme. However, for stability and accuracy enhancements $\partial v^*/\partial x$ and $\partial p^*/\partial y$ can both be discretized at the current R-K stage or, $\partial v^*/\partial x$ at the previous stage and $\partial p^*/\partial y$ at the current stage. The implicit discretization of the pressure derivative is more important for numerical stability. Thus, when the substitution of $(v^{(s)} - v^n)/\Delta t^*$ from Eq. (39) into Eq. (37) is made with $\partial p/\partial y$ evaluated implicitly and $\partial v/\partial x$ evaluated explicitly, we obtain, after rearranging,

$$p^{(s)} + \Delta t^* u_\infty \frac{\partial p^{(s)}}{\partial x} - \frac{a_0 \Delta t^*}{\rho_\infty} \frac{\partial p^{(s)}}{\partial y} = R_p$$
$$= p^n + a_0 \Delta t^* u_\infty \frac{\partial v^{(s-1)}}{\partial x} + \Delta t^* R^{n,n-1,\dots} \quad (40)$$

where $R^{n,n-1,\dots}$ is given by Eq. (38).

It should be noted that the evaluation of $\partial v/\partial x$ also implicitly would result in a second order x derivative in Eq. (40), complicating this equation further. The x derivative of Eq. (40) is discretized using second-order accurate central and the y derivative is discretized using third-order one-sided finite differences. Thus the following tri-diagonal system of equations results on a grid with uniform mesh spacings $\Delta x, \Delta y$:

$$A p^{(s)}_{i-1,jw} + B p^{(s)}_{i,jw} + C p^{(s)}_{i+1,jw} = (R_p)_{i,jw}$$
$$+ \frac{1}{12\Delta y} \frac{a_0 \Delta t^*}{\rho_\infty} (36 p^{(s)}_{i,jw+1} - 18 p^{(s)}_{i,jw+2} + 4 p^{(s)}_{i,jw+3}) \quad (41)$$

where the subscript i signifies the nodal point in the x direction and j signifies the nodal point in the y direction, jw being on the wall, and

$$A = -\frac{u_\infty \Delta t^*}{2\Delta x} \quad (42)$$

$$B = 1 + \frac{22}{12\Delta y} \frac{a_0 \Delta t^*}{\rho_\infty} \quad (43)$$

$$C = \frac{u_\infty \Delta t^*}{2\Delta x} \quad (44)$$

6 Results and Discussion

The above impedance conditions were programmed and tested on CM-5 for one and two-dimensional cases, as a preliminary step towards a fully three-dimensional incorporation into the time-domain, parallel, hybrid ducted fan noise code[1–4] of the present authors. This section presents results that address various numerical issues.

6.1 One-Dimensional Gaussian Pulse

The simplest case to test the time-domain impedance condition is the one-dimensional wave propagation toward an acoustically treated wall. For convenience we use a lowpass filter type impedance at the wall ($x = 0$). We assume the frequency-dependent impedance is given by

$$\frac{Z(\omega)}{\rho_\infty c_\infty} = \frac{1}{1 + t_0 i\omega} \quad (45)$$

where t_0 is a time constant. The impedance is plotted in Fig. 2 for the two different time constants used in this section. The inverse Fourier transform of this impedance function in fact is

$$\frac{Z(t)}{\rho_\infty c_\infty} = \frac{1}{t_0} e^{-t/t_0}, \; t > 0 \quad (46)$$

which is the lowpass filter function chosen in Section 3. The exact z-transform of the time-discrete form of this function is given by Eq. (12). However, we use the backward difference approximation for the $i\omega$ term in the impedance expression to obtain the approximate z-transform of the impedance. Thus we have

$$Z(z) = \frac{\rho_\infty c_\infty/(1 + t_0/\Delta t)}{1 - [(t_0/\Delta t)/(1 + t_0/\Delta t)] z^{-1}} \quad (47)$$

Hence the constants of Eq. (23) are easily identified as

$$\begin{aligned} a_0 &= \rho_\infty c_\infty/(1 + t_0/\Delta t), \\ a_\ell &= 0, \; \ell = 1, 2, \dots, \\ b_1 &= (t_0/\Delta t)/(1 + t_0/\Delta t), \\ b_k &= 0, \; k = 2, 3, \dots \end{aligned} \quad (48)$$

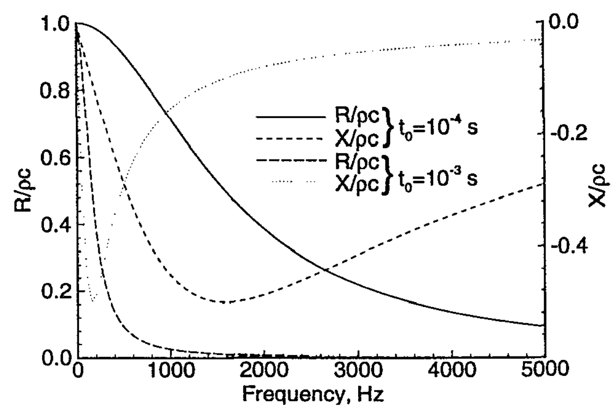

Figure 2: The variation of the specific resistance and reactance of the impedance model, $Z(\omega)/\rho_\infty c_\infty = 1/(1 + t_0 i\omega)$.

Because of its broadband frequency content, a Gaussian pulse is used for the acoustic wave. The solution process involves an implicit wall treatment with $\Delta t^* = \Delta t$ for the acoustic velocity. Figure 3 shows the evolution of the one-dimensional Gaussian pulse. The pulse is split into two components, one propagating to the right and the other propagating to the left. An arrow by a Gaussian indicates the propagation direction. The left propagating component hits the acoustically treated wall with $t_0 = 10^{-4}$ sec. The reduction in the reflected wave amplitude and the deformation in the wave form are evident from the figure. The numerical results are compared with the analytical solution, which is given in the Appendix. The comparisons reveal excellent agreement between the exact solution and the z-transform solution.

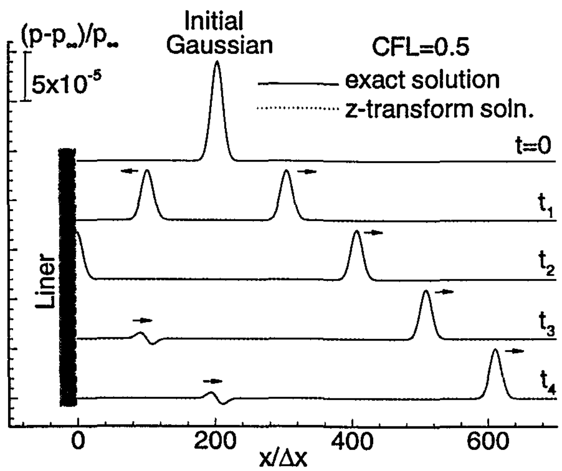

Figure 3: Absorption of a 1D Gaussian pulse by an acoustically treated wall, $Z(\omega)/\rho_\infty c_\infty = 1/(1+10^{-4} i\omega)$.

Since the impedance condition is applied at every R-K stage and the discrete-time-domain impedance condition uses the full time step in its original derivation, it is crucial to examine the effects of the time step size used in the solution of the wall pressures and velocities. This was studied using the same one-dimensional problem with an implicit treatment of the wall velocity. Figure 4 compares three different cases with the exact solution for the reflected Gaussian pressure. The comparisons indicate that if the fractional time step size $(\alpha_s \Delta t)$ is used for the discretization of the normal momentum equation and the full time step (Δt) is used for the impedance model $Z(z)$ given by Eq. (47), the numerical solution does not compare to the exact solution as well as when the full or fractional time step size is used for both the impedance $Z(z)$ and the time-discretized momentum equation. This suggests that the time step size used in the time-discretized impedance condition and the normal momentum equations be consistent.

The question of whether the explicit or implicit discretization of the velocity equation at the wall yields

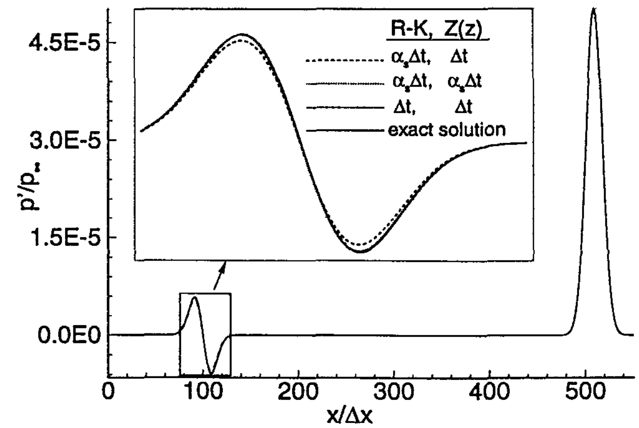

Figure 4: Time step effects on the z-transform solution via the R-K scheme with implicit treatment of wall velocity, $Z(\omega)/\rho_\infty c_\infty = 1/(1+10^{-4} i\omega)$.

more accurate results is answered in Fig. 5, where the z-transform solutions using both approaches are compared with the exact solution for this one-dimensional case. There are essentially no significant differences in the results of the implicit and explicit discretizations for this specific case.

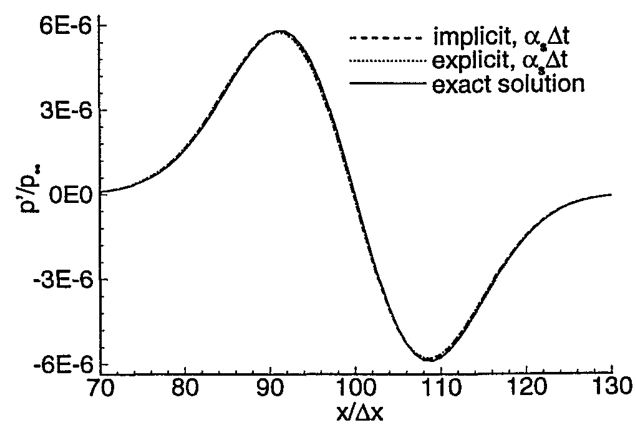

Figure 5: Comparison of the reflected pressures after explicit and implicit treatment of wall velocity, $Z(\omega)/\rho_\infty c_\infty = 1/(1+10^{-4} i\omega)$.

In some cases, however, it was observed that an implicit discretization of the normal momentum equation helps remove the possible instability development at the wall. This fact is shown with an example in Figure 6. For this case the time constant is $t_0 = 10^{-3}$ sec, as opposed to $t_0 = 10^{-4}$ sec of the previous cases. In this particular example increasing this time constant results in an instability development at the wall when the acoustic velocity is obtained using the regular, explicit R-K discretization.

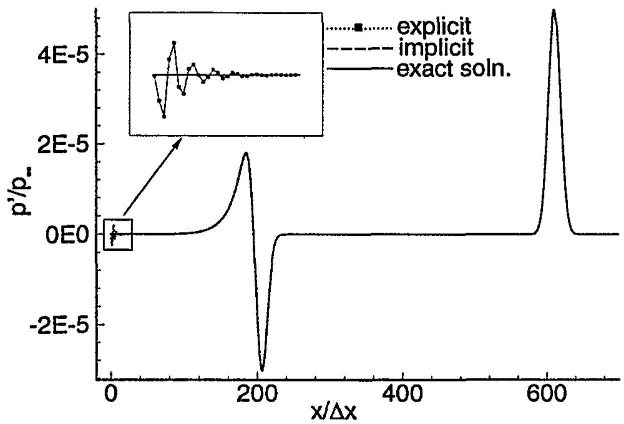

Figure 6: Instability development at the wall in explicit treatment of wall velocity, $Z(\omega)/\rho_\infty c_\infty = 1/(1 + 10^{-3} i\omega)$.

Another very good indicator of how well the z-transform approach works in the present method is to compare the value of the convolution given by Eq. (5) with its recursive approximation given by Eq. (35) using the z-transform. The convolution of Eq. (5) was calculated by a simple summation formula similar to Eq. (8). The same numerical velocities were used in both Eq. (5) and Eq. (35). The evaluation of the convolution used the exact impedance given by Eq. (46). It is evident from Fig. 7 that the right-hand side of Eq. (35) agrees with the exact solution excellently, while the exact convolution (Eq. (5)) lacks accuracy because of the simple summation formula. However, the smaller the time step size (Courant number, CFL), the smaller the error.

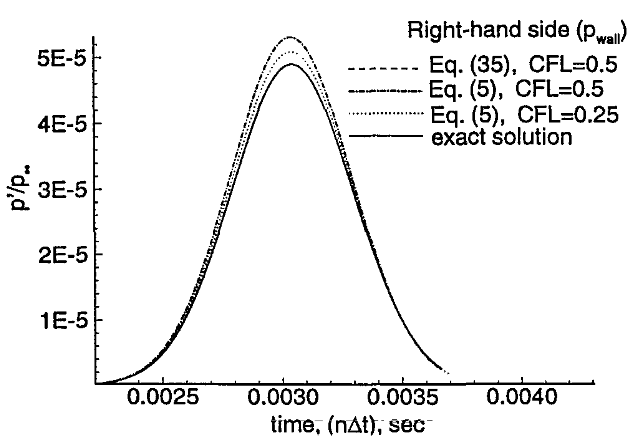

Figure 7: Right-hand sides of Eqs. (5) and (35) (which give the wall pressure) as calculated using the wall pressures and velocities of the z-transform solution, $Z(\omega)/\rho_\infty c_\infty = 1/(1 + 10^{-4} i\omega)$.

6.2 Two-Dimensional Gaussian Pulse

This section discusses two two-dimensional cases. As shown in Fig. 8, a Gaussian pulse is produced at time $t = 0$ above a flat plate over which there could be a uniform flow. The center portion of the flat plate is acoustically treated. Near the edges of the plate hard-wall boundary conditions are used. This was done because of the difficulties encountered with the solution of the impedance condition together with the nonreflecting boundary conditions used. The impedance of the acoustic treatment is assumed to be given by Eq. (45) as in the previous section. The time constant of the impedance model is taken as $t_0 = 10^{-4}$ sec.

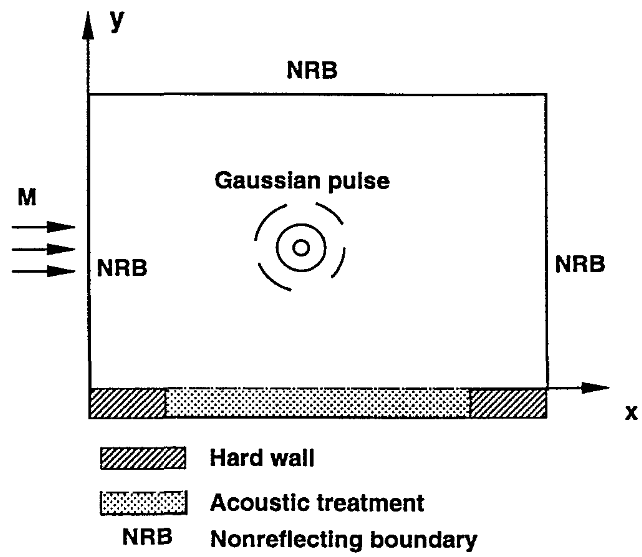

Figure 8: Sketch for the 2D problems.

Figure 9 shows the evolution of the Gaussian pulse for the no-flow case. In this case the convected terms in the impedance condition (Eq. (41)) are zero and no tri-diagonal equation system needs to be inverted. It is evident from the later time solutions that the Gaussian pulse is partially absorbed by the acoustic treatment of the wall.

Figure 10 shows the evolution of the Gaussian pulse for the case with flow. Now the Mach number of the uniform flow is 0.3. Again it is clear from the figure that the acoustic treatment dissipates part of the Gaussian pulse's acoustic energy resulting in lower-amplitude reflected waves. However, it should be indicated that due to the infinitely large jump in the impedance of the wall between the acoustically treated region and the solid wall region (where $Z(\omega) = \infty$), at later time steps an instability developed downstream over the right-hand solid wall. A numerical procedure is needed to circumvent this problem. A gradual transition in impedance could resolve this problem, but the method does not presently

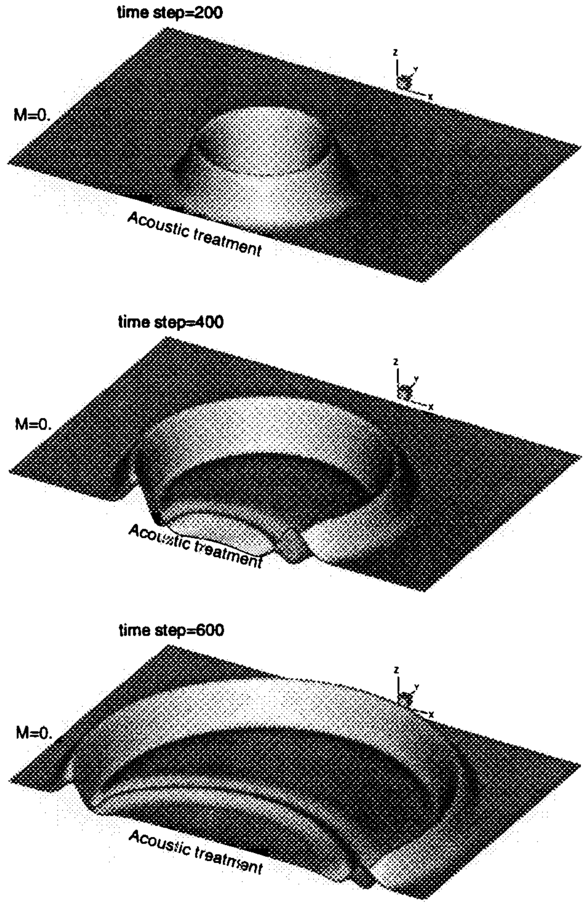

Figure 9: Absorption of a 2D Gaussian pulse by an acoustically treated wall. $M_\infty = 0$, $Z(\omega)/\rho_\infty c_\infty = 1/(1+10^{-4}i\omega)$.

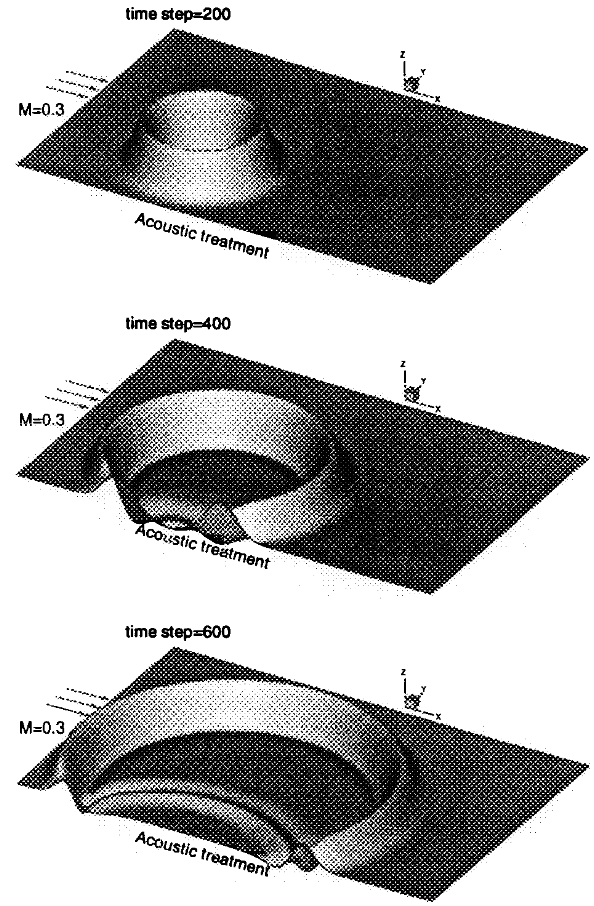

Figure 10: Absorption of a 2D Gaussian pulse by an acoustically treated wall. $M_\infty = 0.3$, $Z(\omega)/\rho_\infty c_\infty = 1/(1+10^{-4}i\omega)$.

allow spatial variations in impedance.

Figure 11 shows the accuracy of the z-transform procedure by comparing the right-hand side of Eq. (7) (convolution) with its recursive approximation, namely the right-hand side of Eq. (37) (half-way on the acoustically treated portion of the wall). Again the convolution was evaluated using the exact impedance and the numerical acoustic velocity as given by the present method. Both results in this case agree very well, indicating that the z-transform procedure is capable of producing accurate results.

7 Conclusions

The time-domain acoustic impedance condition is extremely important for turbofan noise calculations. A time-domain method has been developed using the z-transform from control and signal processing theory. The frequency-domain impedance condition is formulated in the z-domain assuming the impedance is independent of the location on the surface and the impedance is modeled by a rational function in the z-domain. This allows the construction of a digital filter type response function as the approximation to the expensive convolution integral of the time-domain impedance condition. This response function uses the current acoustic velocity input and the previous acoustic pressure outputs and acoustic velocity inputs recursively, reducing the required computations.

The incorporation of this time-discretized impedance condition into the four-stage Runge-Kutta time-integration scheme has been discussed. The solution procedure for the current time step acoustic velocity required by the impedance condition has been discussed. One-dimensional numerical experimentation has revealed that the use of inconsistent time step sizes in the impedance condition and the R-K discretization of the

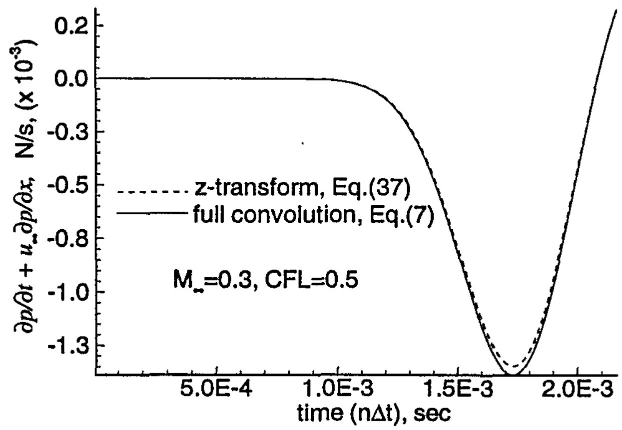

Figure 11: Comparison of the z-transform approximation of the convolution with the numerically calculated exact convolution. $M_\infty = 0.3$, $Z(\omega)/\rho_\infty c_\infty = 1/(1 + 10^{-4} i\omega)$.

normal momentum equation to obtain the acoustic velocity at the wall degrades the accuracy of the results. Also, it has been shown that an implicit time discretization for the acoustic velocity at the wall improves the stability and accuracy characteristics of the present method.

The one and two-dimensional cases with and without flow indicate that the present method is capable of accurately simulating the physical phenomena over acoustically treated walls. Though the present method assumes that the impedance is independent of the location on the surface, it would be useful to add the capability to allow spatial variations in impedance.

Acknowledgments

This work was supported by the NASA Langley Research Center, under the grant NAG-1-1367. The computational resources (CM-5) were provided by the National Center for Supercomputing Applications at the University of Illinois at Urbana-Champaign.

References

[1] Özyörük, Y. *Sound Radiation From Ducted Fans Using Computational Aeroacoustics On Parallel Computers.* Ph.D. thesis, The Pennsylvania State University, December 1995.

[2] Özyörük, Y., and Long, L. N. A new efficient algorithm for computational aeroacoustics on parallel processors. *Journal of Computational Physics*, **125(1)**, pp. 135–149, April 1996.

[3] Özyörük, Y., and Long, L. N. Computation of sound radiating from engine inlets. *AIAA Journal*, **34(5)**, May 1996.

[4] Özyörük, Y., and Long, L. N. Progress in time-domain calculations of ducted fan noise: Multi-grid acceleration of a high-resolution CAA scheme. AIAA Paper 96-1771, 2nd AIAA/CEAS Aeroacoustics Conference, State College, PA, May 1996.

[5] Motsinger, R. E., and Kraft, R. E. Design and performance of duct acoustic treatment. In *Aeroacoustics of Flight Vehicles: Theory and Practice*, NASA Ref. Pub. 1258, vol. 2, 1991.

[6] Eversman, W., Parrett, A. V., Preisser, J. S., and Silcox, R. J. Contributions to the finite element solution of the fan noise radiation problem. *Transactions of the ASME*, **107**, pp. 216–223, 1985.

[7] Oppenheim, A. V., and Schafer, R. W. *Discrete-Time Signal Processing.* Prenctice-Hall, Inc., 1989.

[8] Sullivan, D. M. Frequency-dependent FDTD methods using Z transform. *IEEE Transactions on Antennas and Propagation*, **40(10)**, pp. 1223–1230, October 1992.

[9] Penney, C. *Scattering From Coated Targets Using a Frequency-Dependent Impedance Boundary Condition in the Finite-Difference Time-Domain Method.* Ph.D. thesis, The Pennsylvania State University, University Park, PA, May 1995.

[10] Myers, M. K. On the acoustic boundary condition in the presence of flow. *Journal of Sound and Vibration*, **71(3)**, pp. 429–434, 1980.

[11] Pierce, A. D. *Acoustics –An Introduction to Its Physical Principles and Applications.* Acoustical Society of America, 1989.

[12] Press, W. H., Teukolsky, S. A., Vetterling, W. T., and Flannery, B. P. *Numerical Recipes in Fortran.* Cambridge University Press, second edition, 1992.

[13] Jameson, A., Schmidt, W., and Turkel, E. Numerical solutions of the Euler equations by finite volume methods using Runge-Kutta time-stepping schemes. AIAA Paper 81–1259, 1981.

Appendix

In this section we give the one-dimensional solution of the wave propagation problem in the semi-infinite domain $x \geq 0$. The impedance at the $x = 0$ boundary is given by $Z(\omega)$, and the initial pressure distribution is given by $p_i(x)$. The ambient density is ρ_0 and the ambient speed of sound is c_0. Then the solution for the acoustic pressure at any time $t > 0$ and any $x \geq 0$ is given by

Soft-wall solution:
1) for $x < c_0 t$

$$\begin{aligned} p(t,x) &= \frac{1}{2}p_i(x + c_0 t) - \frac{1}{2}p_i(c_0 t - x) \\ &\quad + \int_{x/c_0}^{t} W(t-\tau)p_i(c_0\tau - x)\, d\tau, \end{aligned} \tag{49}$$

where

$$W(t) = \mathcal{L}_{s:t}^{-1}\left\{\frac{1}{1 + \rho_0 c_0/Z(s)}\right\} \tag{50}$$

in which $\mathcal{L}_{s:t}^{-1}$ is the inverse Laplace transform operator and $Z(s)$ is the Laplace transform of the impedance.

2) for $x > c_0 t$

$$p(t,x) = \frac{1}{2}p_i(x + c_0 t) + \frac{1}{2}p_i(x - c_0 t) \tag{51}$$

Hard-wall solution:
If $Z(s)/\rho_0 c_0 \to \infty$, we obtain the special case (hard-wall) solution as
1) for $x < c_0 t$

$$p(t,x) = \frac{1}{2}p_i(x + c_0 t) + \frac{1}{2}p_i(c_0 t - x) \tag{52}$$

2) for $x > c_0 t$

$$p(t,x) = \frac{1}{2}p_i(x + c_0 t) + \frac{1}{2}p_i(x - c_0 t) \tag{53}$$

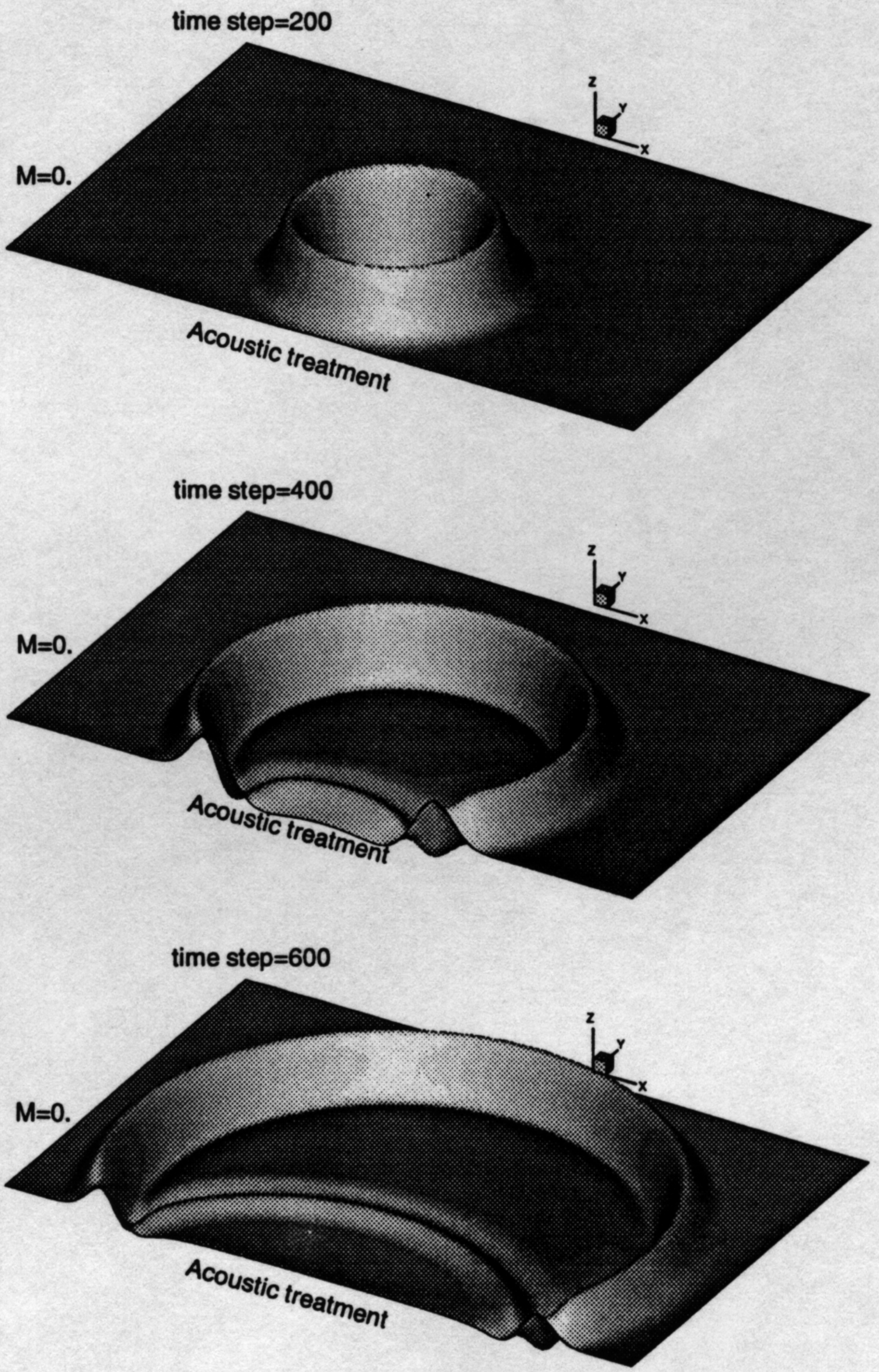

Figure 9: Absorption of a 2D Gaussian pulse by an acoustically treated wall. $M_\infty = 0$, $Z(\omega)/\rho_\infty c_\infty = 1/(1 + 10^{-4} i\omega)$.

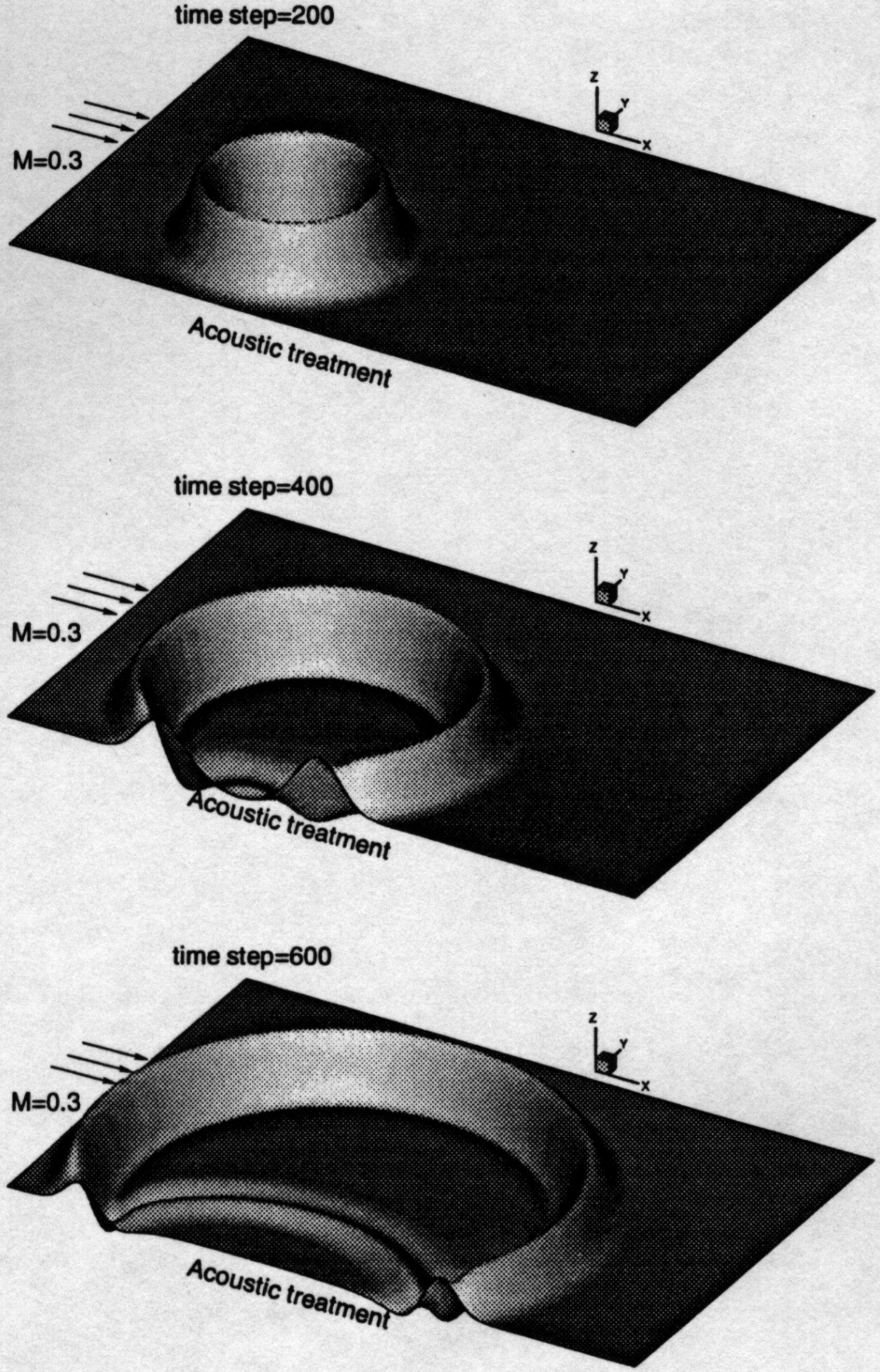

Figure 10: Absorption of a 2D Gaussian pulse by an acoustically treated wall. $M_\infty = 0.3$, $Z(\omega)/\rho_\infty c_\infty = 1/(1+10^{-4}i\omega)$.